

**Dynamics of molecular diffusion of rhodamine 6G in silica nanochannels**Y. Y. Kievsky,<sup>1</sup> B. Carey,<sup>1</sup> S. Naik,<sup>1</sup> N. Mangan,<sup>1</sup> D. ben-Avraham,<sup>1</sup> and I. Sokolov<sup>1,2,a)</sup><sup>1</sup>*Department of Physics, Clarkson University, Potsdam, New York 13699, USA*<sup>2</sup>*NanoBio Laboratory (NABLAB), Clarkson University, Potsdam, New York 13699, USA*

(Received 4 October 2007; accepted 24 March 2008; published online 16 April 2008)

We describe a method to study diffusion of rhodamine 6G dye in single silica nanochannels using arrays of silica nanochannels. Dynamics of the molecules inside single nanochannel is found from the change of the dye concentration in solution with time. A  $10^8$  decrease in the dye diffusion coefficient relative to water was observed. In comparison to single fluorescent molecule studies, the presented method does not require fluorescence of the diffusing molecules. © 2008 American Institute of Physics. [DOI: 10.1063/1.2908875]

Molecular motion, transport/diffusion in well defined nanoscale geometries is of interest not only from fundamental point of view but also from the point of view of applications, such as catalysis, molecular sensing, and controlled drug delivery.<sup>1,2</sup> Recently, a rather fast transport through a single carbon nanotube<sup>3</sup> (CNT) has been reported, which was comparable with the speed of diffusion of water throughout biological water channels. Nanochannels in silica, having a different, hydrophilic nature, are of interest from also the point of view of studying transport in a variety of biological channels,<sup>4,5</sup> the properties of interfacial water,<sup>6–8</sup> capillary of rocks in geophysics,<sup>9–11</sup> etc. While porous silicons<sup>12,13</sup> and silicas have been studied as a host to study diffusion, its nanoporosity either had random geometry or was not well controlled.<sup>6,7</sup> Recently, a single molecule approach was used to study diffusion of some fluorescent molecule in nanoporous silica channels of  $\sim 5$  nm in diameter.<sup>14</sup> Here we report on a new much simpler method to study molecular diffusion in silica nanochannels by using a regular absorption spectroscopy. We apply this method for  $\sim 3$  nm silica nanochannels and rhodamine 6G (R6G) dye molecules. In contrast,<sup>14</sup> our method can be used for nonfluorescent molecules as well.

To study molecular diffusion in a single silica nanochannel, we used the recently synthesized arrays of silica nanochannels (ASNCs).<sup>15</sup> ASNCs were prepared through templated sol-gel process in which silica condensed on the interface of nematic liquid crystals. Each ASNC is a hexagonally shaped fiber, which has approximately 200 000 parallel silica nanochannels, Fig. 1. Each nanochannel has a diameter of 2.9 nm and the length of 4800 nm. The presence of the bulk ordered nanostructure was further confirmed with transmission electron microscopy (TEM) and x-ray diffraction (XRD), (see Fig. 1 in the Supplementary Materials<sup>16</sup>). The location of the peaks of the XRD spectrum corresponds to the hexagonal *p6mm* structure of the ASNCs, having *d* (100) spacing of 36.4 Å. The mean diameter of the channels was obtained from the nitrogen adsorption/desorption measurement.

R6G, a cationic organic dye with a relatively weak hydrogen interaction with silica, is used to study the diffusion inside the nanochannels. To put dye molecules inside nanochannels, we immersed dried ASNCs in a dye solution. The dye solution is soaked inside ASNCs due to the capillary force. To equilibrate any dye gradients, we kept ASNCs in that solution for at least 2000 min. The solution with the suspended ASNCs was placed in a plastic cuvette used for UV-VIS spectroscopy. After precipitation of ASNCs on the cuvette bottom, the excess of the dye solution was removed with a pipette, and a clear solution (medium of the same chemistry but without the dye) was added to the cuvette. At this time the dye started to diffuse out of the nanochannels in the clear solution. (We waited for several hundred minutes to let the initial inhomogeneity in the dye concentration relax. The inhomogeneity was expected due to a slight variation of temperature in the cuvette and because of the mixing of a clear solution with some amount of the dye which remained together with the precipitated ASNCs after removing the soaking solution.) The change of the dye concentration in the clear solution with time due to the diffusion of the dye out of the precipitated ASNCs is measured by the change in absorbance of the solution at the height *h*, Fig. 2. Analyzing such a change, one can obtain the dynamics of the dye molecules per a single nanochannel. Here we study the dye diffusion inside ASNCs immersed in ultrapure water, aqueous acidic solution of hydrochloric acid of pH 1, 1 mM cationic surfactant (cetyltrimethylammonium chloride) solution, and 25% ethanol in water solution. To avoid osmotic pressure stress and the change of chemistry inside the nanochannels, chemistry of both soaking and clear solutions were the same.

When diffusing out of a single ASNC, the dye molecules come from all 200 000 nanochannels. Thus, to find the diffusion from a single nanochannel, the absorbance signal coming from an ASNC should be normalized by the number of nanochannels. To exclude possible artifacts/defects in some ASNCs and to increase the signal level, we study the diffusion out of  $\sim 0.5 \times 10^9$  of ASNCs located at the bottom of a cuvette. It can be done because of a relatively high monodispersity of the synthesized ASNCs ( $\sim 10\%$  rms variability in length<sup>15</sup> and  $\sim 13\%$  in the nanochannel diameters, Fig. 1).

<sup>a)</sup>Author to whom correspondence should be addressed. Electronic mail: isokolov@clarkson.edu.

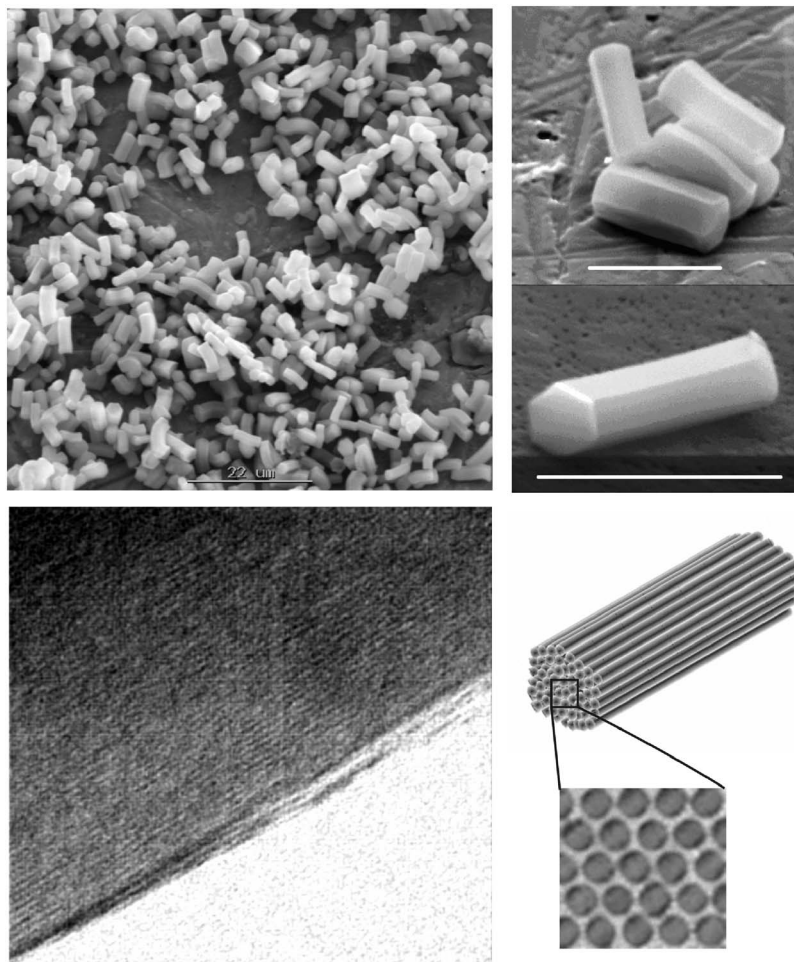


FIG. 1. Top: Scanning electron microscopy image of parallel nanochannels in fiber like ASNC of uniform shape. A large area (left bar size is  $22 \mu\text{m}$ ) and zoom to a few ASNC (right, bar size is  $5 \mu\text{m}$ ). Bottom: TEM image of near the ASNC edge showing a periodicity of about  $3.6 \text{ nm}$  (left); a schematics showing the arrangement of nanochannels in silica matrix (right).

From the theoretical point of view we are dealing with one-dimensional diffusion (a  $1.1 \times 1.5 \text{ nm}^2$  R6G molecule in a  $2.9 \text{ nm}$  channel). To analyze dynamics of the release of the dye molecules from the nanochannels into the surrounding liquid, we make two simplifying assumptions. (1) The density of molecules in the nanochannels is small, so that the

hard core repulsion plays no significant role and the molecules may be regarded as independent, noninteracting diffusers. (2) The concentration level at the surrounding solution is much lower than the initial concentration in the nanochannels, at all times, and we therefore set the concentrations at the edges of the nanochannels to zero. (We have performed a perturbation analysis taking the concentration at the edges into account, finding essentially the same results.)

Let the density of the molecules in one nanochannel be  $\Lambda(x, t)$ , where  $x$  is the location along the nanochannel ( $0 < x < L$ ). The molecules' diffusion inside the nanochannel is described by the classical diffusion equation  $\partial/\partial t \Lambda(x, t) = D \partial^2/\partial x^2 \Lambda(x, t)$ . At the edges of the nanochannels ( $x=0$  and  $x=L$ ) the density of particles is the same as in the solution. Let  $\Lambda_0$  be the initial volume density of the dye molecules in the channels. Keeping the total number of dye molecules constant, and approximating the concentration at the edges to zero, one arrives at the solution of the diffusion equation as follows:

$$\Lambda(x, t) = \Lambda_0 \frac{4}{\pi} \sum_{n=0}^{\infty} \frac{1}{(2n+1)} \times \exp[-2(2n+1)^2 \pi^2 D t / L^2] \sin[(2n+1) \pi x / L]. \quad (1)$$

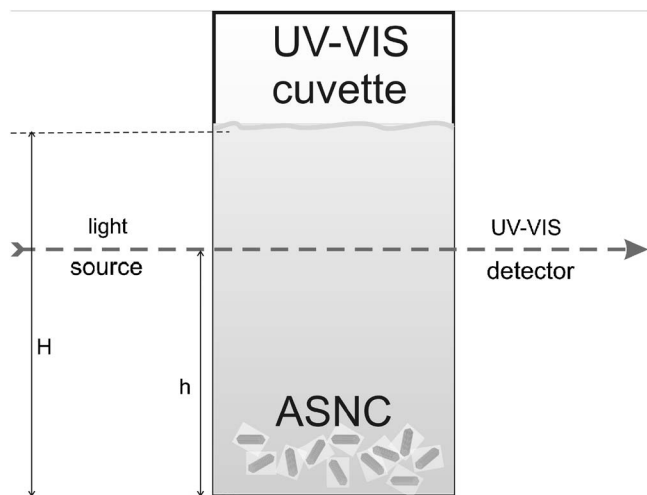


FIG. 2. Schematics of the measurements of the concentration of the dye diffusing out of the nanochannels of ASNCs. Dye concentration in the cuvette was measured by using Beer's law, which relates the concentration and absorbance.

We can now compute how much dye absorbs the light passing through the solution at height  $h$ , Fig. 2. The nanochannels “inject” dye into the solution at the rate

$$f(t) \equiv \left| D \frac{\partial}{\partial x} \Lambda(x, t) \right|_{x=0, L} \\ = \alpha \frac{4D\Lambda_0}{L} \sum_{n=0}^{\infty} \exp[-2(2n+1)^2 \pi^2 D t / L^2], \quad (2)$$

where  $\alpha$  is the ratio of the area of all nanochannels to the area of the cuvette. This dye diffuses in the liquid to height  $h$  with diffusion constant  $D_{\text{free}}$  (this value is taken hereafter to be  $2.8 \times 10^8 \text{ nm}^2/\text{s}$ , and virtually independent of the aqueous media used in this study, see, e.g., Refs. 17–20). We take the reflecting boundary conditions at heights zero and  $H$ , Fig. 2, because the dye cannot diffuse above the liquid (at height  $H$ ) and below the cuvette bottom (at height zero). Thus, the dye concentration in the solution  $\rho(h, t)$  at height  $h$  reads

$$\rho(h, t) = \rho(t=0) + \int_0^t G(h, t-t') f(t') dt', \quad (3)$$

where the Green’s function is

$$G(h, t) = \frac{2}{\sqrt{4\pi D_{\text{free}} t}} \left[ \exp\left(-\frac{h^2}{4D_{\text{free}} t}\right) + \sum_{m=2}^{\infty} \left( \exp\left(-\frac{(h-mH)^2}{4D_{\text{free}} t}\right) + \exp\left(-\frac{(h+mH)^2}{4D_{\text{free}} t}\right) \right) \right]. \quad (4)$$

Factor 2 in front of the integral comes from the two open ends of the nanochannels. A small concentration  $\rho(t=0)$  presents due to some initial amount of the dye which remained together with the precipitated ASNCs after removing the soaking solution, as was noted in the experiment description. In principle, the integral in Eq. (3) can be taken in special functions. However, to avoid unnecessary mathematics, we will numerically treat Eq. (3) when fitting experimental data.

Figure 3 shows the measured concentrations of the dye in the cuvette shown in Fig. 2 as a function of time. Results of fitting the data with Eq. (3) are also shown with solid lines. The fitting was done with respect to the initial concentration [parameters  $\Lambda_0, \rho(t=0)$ ] and the coefficient of diffusion in nanochannels  $D$ . (In our experimental design we had  $H=3 \text{ cm}$ ,  $h=1.1 \text{ cm}$  for water, acid, and surfactant, and  $h=1.3 \text{ cm}$  for the ethanol solution cuvettes. The width of the light beam is about  $0.1 \text{ cm}$ . It can be taken into account by integrating Eq. (3) over  $h$  in that range. The difference is, however, quite small, and therefore, it was not done here.) One can see that the model works very well. The fitting parameters are collected in Table I. The method restricts the fitted coefficients of diffusion to the values shown in Table I within less than 5%, except the case of surfactant. Diffusion in this case is relatively fast. It could be confused with the free diffusion of the dye through distance  $h$  (Fig. 2). This case is discussed in detail in the Supplementary Materials.<sup>16</sup>

To understand if the obtained concentration  $\Lambda_0$  is reasonable, we estimated the initial number of molecules per nanochannels and the initial average distance between mol-

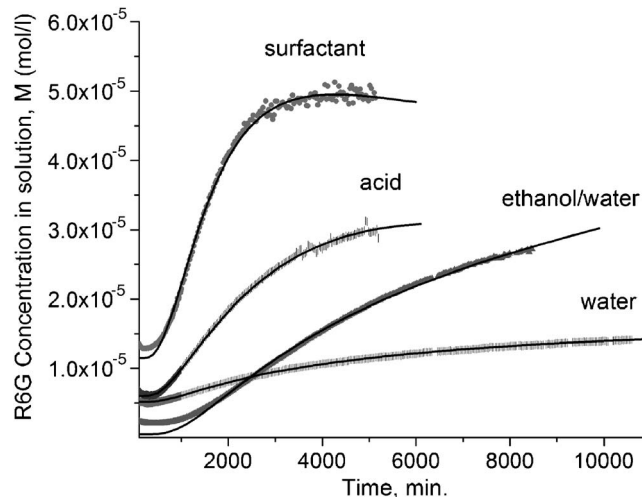


FIG. 3. Measured concentrations of the dye molecules diffused out of ASNCs in water, 1 mM surfactant solution, 25% ethanol in water solution, and acidic aqueous solution with pH 1. Solid lines are the model [Eq. (3)] fits. The initial number of molecules per nanochannel is found by multiplying  $\Lambda_0$  by the volume of each ASNC.

ecules in each nanochannels, Table I. Comparing the diffusion coefficient of free R6G dye in water,<sup>17</sup>  $2.8 \times 10^8 \text{ nm}^2/\text{s}$ , with that presented in Table I, one can see a very strong effect of confinement, eight orders of magnitude decrease for diffusion in water. A decrease in  $\sim 100$  times with respect to the free dye diffusion was previously observed for spherical silica gel particles (effective pore diameter was  $6.5 \text{ nm}$ ).<sup>21</sup>  $8 \times 10^3 \text{ cm}^2/\text{s}$  diffusion coefficient was observed<sup>22</sup> for R6G coming out of nano(meso)porous silica spheres (effective pore diameter was not reported but can be estimated as  $\sim 3 \text{ nm}$ ) at  $50 \text{ }^\circ\text{C}$  temperature. For small molecules exhibiting no detectable adsorption to silica surfaces, diffusion rates within the intraparticle micropores (no specific pore diameter was estimated) of silica have been estimated to be  $\sim 10 \text{ nm}^2/\text{s}$ , which is close to the observed here.<sup>23</sup>

It should be noted that our results are quite different from the recently reported data on the diffusion in CNTs,<sup>3</sup> in which the diffusion of water and hydrocarbons through  $7 \text{ nm}$  CNTs was significantly faster than in solution. This was attributed to hydrophobicity of carbon wall which leads to effectively frictionless surface inside CNT. In contrast with CNT, silica surface of nanochannels is hydrophilic, and has active hydroxide groups. A straightforward reason to explain the observed decrease in the diffusion coefficient would be a strong interaction of the dye molecules with the silica wall. As was reported in Ref. 24 for the case of functionalized CNT, such an interaction results in a “tipping effect,” a situation when the diffusant molecules clog the open ends of the nanochannels. In our case, we demonstrate the absence of this effect in the Supplementary Materials.<sup>16</sup>

We will now discuss the role of the electrostatic interaction, which is expected to be the strongest one among other possible interactions (van der Waals and hydrogen interactions) between the dye molecules and the silica wall. Dye molecules carry one positive electron charge in neutral aqueous environment, and positive double electron charge in the

TABLE I. Fitting parameters for Eq. (3): constants  $\rho(t=0)$ ,  $\Lambda_0$ , diffusion coefficient  $D$ . The initial average distance between the molecules inside each nanochannel was found as the initial number of molecules per nanochannel divided by the nanochannel length.

	$\rho(t=0)$ $10^{-6}M$	$\Lambda_0$ (mM)	$D$ ( $\text{nm}^2/\text{s}$ )	Initial averaged distance between molecules (nm)	Initial No. of molecules/nanochannel
R6G in water	5.2	2.0	2.9	30	160
R6G in pH 1	6.0	9.5	9.8	6	780
R6G in EtOH	0.5	20	0.49	3	1600
R6G in CTACl	11	6.6	40	9	540

solutions with higher acidities. Because of the negative charge on silica surface (for the acidity of  $\text{pH} > 3$ ), we expect the dye physisorbed on silica in neutral  $\text{pH}$  due to the electrostatic interaction. For  $\text{pH} < 2$ , we expect a weak or no physisorption due to the electrostatic repulsion between the dye and silica surfaces, which is positively charged in that case. Comparing these two cases, one can see from Table I that the diffusion coefficient indeed increases more than three times for the acidic environment of  $\text{pH} 1$ . However, it is still about eight orders of magnitude smaller than in just water solution.

One can see from Table I that the diffusion coefficient in the ethanol solution inside the channels decreases six times compared to that in water. As was reported,<sup>25</sup> the surface charge on the silica surface decreases  $\sim 10\%$ . On the other hand,  $\sim 20\%$  drop in dielectric constant ethanol-water mixture as compared to water should result in the increase in the dye surface interaction and, consequently, in the drop in the diffusion coefficient. The observed decrease could also be related to a strong suppression of the diffusion in confined organic solvents, see, e.g., Refs. 26 and 27.

An interesting behavior can be observed in the case of surfactant medium. One can clearly see quite a large increase in the diffusion coefficient,  $\sim 13$  times greater than in water. This phenomenon is presumably related to the adsorption of the surfactant molecules on the silica wall of the nanochannels. Such absorption is expected because those molecules formed the template when self-assembling the ASNCs.<sup>15</sup> To some extent, the inner surface of the nanochannels carries molecular imprint of the headgroups of surfactant molecules. Positive charges of the surfactant headgroups may also help to attract the molecules to the negatively charged silica surface. Moreover, because of the strong hydrophobicity of surfactant tails, surfactant molecules form into the cylindrical micelles inside the silica nanochannels.<sup>28</sup> As seen from Raman spectra of the ASNCs (not shown), the surfactant molecules stay inside of the ASNCs after the dye molecules diffuse out. This is indicative of hydrophobic phase separation and micelle formation inside the channels. Thus, the surfactant can act in two different ways on the dye diffusion: It decreases electrostatic dye-wall interaction by shielding negatively charged silica wall and it helps to expel hydrophilic dye from the inside of hydrophobic surfactant tails located inside the nanochannels. This is somewhat similar to the increase in diffusion of hydrophilic molecules in hydrophobic environment of CNT.<sup>3</sup> As we previously saw, the effect of electrostatic interaction did alter the diffusion coefficient three times only. Hence, we can conclude that the

presence of surfactant hydrophobic tails, creating hydrophobic environment inside the nanochannels, helps dye molecules to diffuse out faster.

Hydrophobic and electrostatic interactions are typically by an order of magnitude stronger than other hydrogen and van der Waals<sup>29</sup> interactions existing between the dye and silica. Hydrophobic environment of the nanochannels created with the surfactant molecules increases the coefficient of diffusion by a factor of 13, whereas inversion of electrostatic interaction changes the diffusion coefficient by a factor of 3. Thus, we can conclude that the obtained eight-orders-of-magnitude decrease in the diffusion of the dye inside silica nanochannels can unlikely be explained, at least, only by interaction of the dye molecules with the silica wall.

The other factor that could decrease diffusion is a physical confinement of the molecules inside the channels, i.e., hindered diffusion.<sup>30-32</sup> Pure steric interactions between the dye and the pore wall lead to the hindered diffusivity. According to Renkin's equation,<sup>33</sup> the diffusion coefficient due to this effect decreases by a factor of

$$\alpha = (1 - \lambda)^2(1 - 2.104\lambda + 2.09\lambda^3 - 0.95\lambda^5), \quad (5)$$

where  $\lambda$  is the ratio of the molecular to the pore radii. Using the size of the dye molecule (1.5 nm, its maximum steric diameter) and diameter of the nanochannels (2.9 nm), one can see that the decrease in the diffusion coefficient cannot exceed two orders of magnitude. However, as was shown in Ref. 32, the diffusion coefficient can indeed drop virtually to zero in the case of hindered diffusivity of molecules interacting with cylindrical pore (it was shown for a case of charged spherical particle in a cylindrical pore). Presumably we are dealing with a similar diffusion here, the observed considerable decrease in the diffusion comes from a synergetic action of both physical confinement of the molecules inside the nanochannels and their interaction with the nanochannels. The existing theoretical models of diffusion, however, are not accurate enough to take into account interaction of a R6G molecule and the silica wall. This is because the charge distribution on R6G molecule is highly inhomogeneous. This will definitely change the electrostatic interaction between the dye and silica surface. To understand the nature of the observed diffusion in a more quantitative way, molecular dynamics modeling is needed.

Support is acknowledged by I.S. from the ARO (W911NF-05-1-0339) and by D.b-A. from the NSF-(PHY0555312). Correspondence and requests for material should be addressed to I.S.

- <sup>1</sup>C. R. Martin and P. Kohli, *Nat. Rev. Drug Discovery* **2**, 29 (2003).
- <sup>2</sup>M. E. Davis, *Nature (London)* **364**, 391 (1993).
- <sup>3</sup>M. Majumder, N. Chopra, R. Andrews, and B. J. Hinds, *Nature (London)* **438**, 44 (2005).
- <sup>4</sup>M. S. P. Sansom, I. D. Kerr, J. Breed, and R. Sankararamkrishnan, *Biophys. J.* **70**, 693 (1996).
- <sup>5</sup>R. M. LyndenBell and J. C. Rasaiah, *J. Chem. Phys.* **105**, 9266 (1996).
- <sup>6</sup>P. Gallo, M. Rovere, M. A. Ricci, C. Hartnig, and E. Spohr, *Europhys. Lett.* **49**, 183 (2000).
- <sup>7</sup>P. Gallo, M. Rovere, and E. Spohr, *Phys. Rev. Lett.* **85**, 4317 (2000).
- <sup>8</sup>A. Poynor, L. Hong, I. K. Robinson, S. Granick, Z. Zhang, and P. A. Fenter, *Phys. Rev. Lett.* **97**, 266101 (2006).
- <sup>9</sup>C. L. Perrin, P. M. Tardy, K. S. Sorbie, and J. C. Crawshaw, *J. Colloid Interface Sci.* **295**, 542 (2006).
- <sup>10</sup>A. P. Radlinski, M. A. Ioannidis, A. L. Hinde, M. Hainbuchner, M. Baron, H. Rauch, and S. R. Kline, *J. Colloid Interface Sci.* **274**, 607 (2004).
- <sup>11</sup>Y. Q. Song, S. Ryu, and P. N. Sen, *Nature (London)* **406**, 178 (2000).
- <sup>12</sup>A. Khokhlov, R. Valiullin, J. Karger, F. Steinbach, and A. Feldhoff, *New J. Phys.* **9**, 272 (2007).
- <sup>13</sup>R. Valiullin, P. Kortunov, J. Karger, and V. Timoshenko, *J. Chem. Phys.* **120**, 11804 (2004).
- <sup>14</sup>A. Zurner, J. Kirstein, M. Doblinger, C. Brauchle, and T. Bein, *Nature (London)* **450**, 705 (2007).
- <sup>15</sup>Y. Kievsky and I. Sokolov, *IEEE Trans. Nanotechnol.* **4**, 490 (2005).
- <sup>16</sup>See EPAPS Document No. E-JCPSA6-128-036816 for further details on structure of nanochannels, diffusion analysis, and evidence against the tipping effect. For more information on EPAPS, see <http://www.aip.org/pubservs/epaps.html>.
- <sup>17</sup>S. M. Nie, D. T. Chiu, and R. N. Zare, *Science* **266**, 1018 (1994).
- <sup>18</sup>R. L. Hansen, X. R. Zhu, and J. M. Harris, *Anal. Chem.* **70**, 1281 (1998).
- <sup>19</sup>C. T. Culbertson, S. C. Jacobson, and J. M. Ramsey, *Talanta* **56**, 365 (2002).
- <sup>20</sup>K. Ibuki and M. Nakahara, *J. Chem. Phys.* **84**, 2776 (1986).
- <sup>21</sup>T. Sekine and K. Nakatani, *Langmuir* **18**, 694 (2002).
- <sup>22</sup>Q. Fu, G. V. R. Rao, L. K. Ista, Y. Wu, B. P. Andrzejewski, L. A. Sklar, T. L. Ward, and G. P. Lopez, *Adv. Mater. (Weinheim, Ger.)* **15**, 1262 (2003).
- <sup>23</sup>D. Rivera and J. M. Harris, *Anal. Chem.* **73**, 411 (2001).
- <sup>24</sup>J. Kirstein, B. Platschek, C. Jung, R. Brown, T. Bein, and C. Brauchle, *Nat. Mater.* **6**, 303 (2007).
- <sup>25</sup>J. Ren, S. Song, A. Lopez-Valdivieso, J. Shen, and S. Lu, *J. Colloid Interface Sci.* **238**, 279 (2001).
- <sup>26</sup>U. Raviv, P. Laurat, and J. Klein, *Nature (London)* **413**, 51 (2001).
- <sup>27</sup>M. C. Bellissent-Funel, *Eur. Phys. J. E* **12**, 83 (2003).
- <sup>28</sup>G. A. Ozin and A. Arsenault, *Nanochemistry: A Chemical Approach to Nanomaterials* (Royal Society of Chemistry, London, 2005).
- <sup>29</sup>J. Israelachvili, *Intermolecular and Surface Forces*, 2nd ed. (Academic, San Diego, 1992).
- <sup>30</sup>B. D. Bath, H. S. White, and E. R. Scott, *Anal. Chem.* **72**, 433 (2000).
- <sup>31</sup>W. M. Deen, *AIChE J.* **33**, 1409 (1987).
- <sup>32</sup>F. G. Smith and W. M. Deen, *J. Colloid Interface Sci.* **91**, 571 (1983).
- <sup>33</sup>E. M. Renkin, *J. Gen. Physiol.* **38**, 225 (1954).